Computational Modelling of Concrete Structures, de Borst, Bićanić, Mang & Meschke (eds)
© 1998 Balkema, Rotterdam, ISBN 90 5410 946 7

An elasto-damage constitutive model for high-strength concrete

A. R. Khan, A. H. Al-Gadhib & M. H. Baluch
Department of Civil Engineering, King Fahd University of Petroleum and Minerals, Dhahran, Saudi Arabia

ABSTRACT: A constitutive model for normal and high strength concrete is proposed within the framework of continuum damage mechanics (CDM). The proposed model makes use of the damage effect tensor $\underline{M}$, and the concept of bounding surface for constitutive relations and evolution of damage. Essential features of concrete such as degradation of elastic properties, strain softening, gain in strength under increasing confinement and different behavior in tension and compression have been captured effectively. Predicted results compare well with the experimental results.

1 INTRODUCTION

In recent years considerable research has been focused on modelling of mechanical behavior of concrete. The mechanical behavior of concrete is very complicated and the possible variations in material characteristics have not been modelled effectively under various theoretical frameworks such as non-linear elasticity, rate-independent plasticity, endochronic theory and plastic fracturing theory. More recently, the theory of continuum damage mechanics (CDM) originally proposed by Kachanov (1958) has been applied to concrete by different researchers. Highly oriented cracking occurring in concrete under loading is modelled by the researchers using scalar, vectorial/tensorial damage variables.

Continuum damage theory for the general case of anisotropic damage in a consistent mathematical and mechanical framework was cast by using damage effect tensor $\underline{M}$ by Chow and Wang (1987a, b), but their work was limited to metals. The concept of bounding surface first applied to metals by Dafalias & Popov (1977), was applied to concrete by Fardis et al. (1983), Suaris et al. (1990), Voyiadjis & Abu-Lebdeh (1993), Abu-Lebdeh & Voyiadjis (1993), Yazdani & Schreyer (1990).

In the present work, the effective compliance matrix $[\tilde{C}]$ is derived by using the damage effect tensor which takes into account the different behavior of concrete in tension and compression by introducing two parameters α and β. Damage growth is derived using a concept similar to the bounding surface as proposed by Suaris et al. (1990). In this method, three surfaces, namely, a limit fracture surface (which defines the onset of damage), a loading surface and a bounding surface are defined. Damage growth would occur only when the loading surface is outside of the limit fracture surface.

1.1 *Damage effect tensor*

Based on the theory of continuum damage mechanics, the effective Cauchy stress tensor $\tilde{\sigma}$ is related to the usual Cauchy stress tensor σ by

$$\tilde{\sigma} = \frac{\sigma}{1-\omega} \tag{1}$$

For the anisotropic damage, the effective stress may be expressed in a generalized form as

$$\tilde{\sigma} = M(\omega) : \sigma \tag{2}$$

where the symbol (:) means the tensorial product contracted on two indices, and $M(\omega)$ known as damage effect tensor is a linear symmetric operator represented by a fourth order tensor. When the principal axes of effective stresses $\tilde{\sigma}$ and material damage during loading are assumed to coincide with the conventional stresses σ, the components of $\tilde{\sigma}$ may be expressed in the principal coordinate system as

$$\tilde{\sigma}_i = M_{ij}(\omega)\sigma_j \tag{3}$$

One of the simplest forms is to introduce material damage in the principal directions only (Chow & Wang, 1987a, b). One obvious criterion for developing such a generalized form of the damage effect tensor is that it should be reduced to a scalar for isotropic damage. Based on phenomenological evidence and satisfaction of the above criterion, following damage effect tensor for concrete, $M(\omega)$, is developed and expressed in the principal coordinate system as:

$$M_{ij}(\omega) = 0, \; i \neq j$$

$$M_{11} = \frac{(1-\beta\omega_1)}{(1-\alpha\omega_1)(1-\beta\omega_2)(1-\beta\omega_3)}$$

$$M_{22} = \frac{(1-\beta\omega_2)}{(1-\alpha\omega_2)(1-\beta\omega_3)(1-\beta\omega_1)} \qquad (4)$$

$$M_{33} = \frac{(1-\beta\omega_3)}{(1-\alpha\omega_3)(1-\beta\omega_1)(1-\beta\omega_2)}$$

where ω_i, i = 1,2,3, are the principal damage components. The parameters α and β are introduced to capture the different behavior of concrete in tension and compression.

It is obvious from (4) that for isotropic damage when $\omega_1 = \omega_2 = \omega_3 = \omega$, the proposed M-tensor can be readily reduced to a scalar.

1.2 *Effective compliance matrix*

Effective compliance matrix for damaged material in the principal coordinate system is derived using the elastic energy equivalence concept as proposed by Cordebois & Sidoroff (1982), who postulated that the complementary elastic energy for a damaged material is the same in form as that of an undamaged material, except that the stress is replaced by the effective stress in the energy formulation. Since the complementary elastic energy $\Lambda^e(\sigma,0)$ of an undamaged material ($\omega = 0$) is

$$\Lambda^e(\sigma,0) = \frac{1}{2}\,\sigma^T : C : \sigma \qquad (5)$$

The complementary energy of a damaged material can be expressed as

$$\Lambda^e(\sigma,\omega) = \Lambda^e(\tilde{\sigma},0) = \frac{1}{2}\,\tilde{\sigma}^T : C : \tilde{\sigma}$$

$$= \frac{1}{2}\,\sigma^T : (M^T : C : M) : \sigma$$

$$= \frac{1}{2}\,\sigma^T : \tilde{C} : \sigma \qquad (6)$$

where,

$$\tilde{C} = M^T : C : M \qquad (7)$$

The linear elastic stress-strain equation for damaged material may be written as

$$\varepsilon^e = \frac{\partial \Lambda^e(\sigma,\omega)}{\partial \sigma} = (M^T : C : M) : \sigma = \tilde{C} : \sigma \qquad (8)$$

The compliance matrix, [C], for isotropic materials in the principal coordinate system is

$$[C] = \frac{1}{E_o}\begin{bmatrix} 1 & -\nu & -\nu \\ -\nu & 1 & -\nu \\ -\nu & -\nu & 1 \end{bmatrix} \qquad (9)$$

Substituting (9) and (4) in (7), effective compliance matrix for damaged material in the principal coordinate system is expressed as

$$\tilde{C}_{11} = \frac{(1-\beta\omega_1)^2}{(1-\alpha\omega_1)^2(1-\beta\omega_2)^2(1-\beta\omega_3)^2}$$

$$\tilde{C}_{12} = \tilde{C}_{21} = \frac{-\nu}{(1-\alpha\omega_1)(1-\alpha\omega_2)(1-\beta\omega_3)^2}$$

$$\tilde{C}_{13} = \tilde{C}_{31} = \frac{-\nu}{(1-\alpha\omega_1)(1-\alpha\omega_3)(1-\beta\omega_2)^2} \qquad (10)$$

$$\tilde{C}_{22} = \frac{(1-\beta\omega_2)^2}{(1-\alpha\omega_2)^2(1-\beta\omega_3)^2(1-\beta\omega_1)^2}$$

$$\tilde{C}_{23} = \tilde{C}_{32} = \frac{-\nu}{(1-\alpha\omega_2)(1-\alpha\omega_3)(1-\beta\omega_1)^2}$$

$$\tilde{C}_{33} = \frac{(1-\beta\omega_3)^2}{(1-\alpha\omega_3)^2(1-\beta\omega_1)^2(1-\beta\omega_2)^2}$$

From (10) it is obvious that the thermodynamic constraint requirement $E_i\,\nu_{ji} = E_j\,\nu_{ij}$ is satisfied.

1.3 *Bounding surface*

In order to construct a rational model accounting for damage growth, concepts are borrowed from incremental theory of plasticity in general and the bounding surface plasticity model in particular as introduced by Dafalias & Popov (1977). Plasticity bounding surface model as proposed by Dafalias

requires definition of multiple surfaces in stress space. However, the fundamental surfaces in the present work are best described in strain-energy release space, as proposed by Suaris et al. (1990)

$$f = (R_i R_i)^{1/2} - R_c / b = 0 \tag{11}$$

$$F = (\bar{R}_i \bar{R}_i)^{1/2} - R_c = 0 \tag{12}$$

$$f_o = (R_i R_i)^{1/2} - R_o = 0 \tag{13}$$

where, f is the loading function surface, F is the bounding surface, f_o is a limit fracture surface (Suaris et al. 1990). The loading function surface (f) is defined in terms of thermodynamic-force conjugates, R_i, where,

$$R_i = \rho \frac{\partial \Lambda}{\partial \omega_i}(\sigma_{ij}, \omega_i) \tag{14}$$

$\bar{R}_i$ is an image point on $F = 0$ associated with a given point R_i on $f = 0$ defined by a mapping rule

$$\bar{R}_i = b R_i \tag{15}$$

$$b = R_c / (R_i R_i)^{1/2} \tag{16}$$

with the mapping parameter b ranging from an initial value of ∞ to a limiting value of 1 on growth of loading surface to coalesce with bounding surface. R_c, critical strain energy release rate, is a parameter of the model and is calibrated to the standard uniaxial compression test, and is suggested to be 1.29. R_o defines the initiation of microcracking which occurs at about 40% of the peak stress as indicated by experimental results, and it varies with the compressive strength of concrete as:

$$R_o = \sqrt{2}\beta\ (0.4 f_c')^2 / E_o \tag{17}$$

Damage is hypothesized to accumulate at levels of strain energy release rate resulting in the loading surface (f) traversing the limit fracture surface (f_o) and rupture in the damage sense is said to occur when 'f' grows large enough to coalesce with the bounding surface F fixed in the R_i space.

It can be argued from the above discussion that R_c should also vary with the compressive strength of concrete, f_c', like R_o. At this point it seems appropriate to discuss the role of parameters α and β. It is true that R_c will vary with f_c', but with the introduction of α and β it does not matter that R_c is fixed or varying. α and β control the movement of the loading surface which describes the onset of damage or failure, i.e. higher values of α and β means faster movement of loading surface and hence lower peak stress, as it will reach the bounding surface much earlier than with lower values of α and β. This makes the model flexible enough to accommodate normal as well as high strengths of concrete.

1.4 *Damage evolution*

The damage growth is determined from the loading surface, f, as

$$d\omega_i = d\lambda \frac{\partial f}{\partial R_i} \tag{18}$$

With $k = R_c/b$, equation of loading becomes

$$f(R_i, k) = (R_i R_i)^{1/2} - k(\bar{\omega}_p) = 0 \tag{19}$$

where ω_p, the norm of accumulated damage is defined as,

$$d\bar{\omega}_p = C(d\omega_i\, d\omega_i)^{1/2} \quad (C \text{ is constant}) \tag{20}$$

Consistency condition $df = 0$

$$\frac{\partial f}{\partial R_i} dR_i + \frac{\partial f}{\partial k} dk = 0 \tag{21}$$

From (14)

$$dR_i = \frac{\partial R_i}{\partial \sigma_k} d\sigma_k + \frac{\partial R_i}{\partial \omega_j} d\omega_j \tag{22}$$

Substituting in (21)

$$\frac{\partial f}{\partial R_i}\left(\frac{\partial R_i}{\partial \sigma_k} d\sigma_k + \frac{\partial R_i}{\partial \omega_j} d\omega_j\right) + \frac{\partial f}{\partial k}\frac{\partial k}{\partial \bar{\omega}_p} d\bar{\omega}_p = 0 \tag{23}$$

Substituting (18) in (20)

$$d\bar{\omega}_p = C\left(d\lambda \left(\frac{\partial f}{\partial R_i}\frac{\partial f}{\partial R_i}\right)^{1/2}\right) \tag{24}$$

It can be shown that $\left(\frac{\partial f}{\partial R_i}\frac{\partial f}{\partial R_i}\right)^{1/2} = 1$ and for $C = 1$

$$d\bar{\omega}_p = d\lambda \tag{25}$$

Using (18), (19) and (25) in (24) and solving for $d\lambda$ yields

$$d\lambda = \frac{\frac{\partial f}{\partial R_i}\frac{\partial R_i}{\partial \sigma_k} d\sigma_k}{\frac{\partial k}{\partial \bar{\omega}_p} - \frac{\partial f}{\partial R_i}\frac{\partial R_i}{\partial \omega_j}\frac{\partial f}{\partial R_j}} \tag{26}$$

Introducing $H = \dfrac{\partial k}{\partial \bar{\omega}_p}$ = damage modulus, it can be measured experimentally in a uniaxial compression test and the same form is assumed for more general stress paths.

In the present work, H is expressed as a function of the distance between the loading and the bounding surface, given by

$$H = \frac{D\delta}{\langle \delta_{in} - \delta \rangle} \tag{27}$$

where $D = 2.65$ is a constant and $< >$ are Macaulay brackets that set the quantity within it to zero if the value is negative. The normalized distance δ between the loading and bounding surfaces is given by

$$\delta = 1 - \frac{1}{b} \tag{28}$$

$\delta = \delta_{in}$ corresponds to R_o when the loading surface first crosses the limit fracture surface (Suaris et al. 1990).

2 INCREMENTAL STRESS-STRAIN RELATIONS

2.1 *Elasto-damage compliance matrix*

Total form of stress-strain law can be expressed as

$$\varepsilon_i = C_{ij}(\omega_i)\sigma_j \tag{29}$$

The incremental form of Equation (29) is given by

$$d\varepsilon_i = C_{ij}\, d\sigma_j + \sigma_j \frac{\partial C_{ij}}{\sigma \omega_k} d\omega_k \tag{30}$$

or

$$d\varepsilon_i = C_{ij}\, d\sigma_j + \sigma_j \frac{\partial C_{ij}}{\sigma \omega_k} d\lambda \frac{\partial f}{\partial R_k} \tag{31}$$

$$d\varepsilon_i = \left\{ C_{ij} + \sigma_j \frac{\partial C_{ij}}{\partial \omega_k}\frac{\partial f}{\partial R_k} d\lambda \right\} d\sigma_j \tag{32}$$

or

$$d\varepsilon_i = C_{ij}^{ed}\, d\sigma_j \tag{33}$$

where $d\lambda$ is defined in Equation (26).

where C_{ij}^{ed} is the elasto-damage compliance matrix as defined in Equation (32). Equation (33) is useful in a stress control testing.

2.2 *Elasto-damage stiffness matrix*

The constitutive equation for strain control can be expressed as

$$\sigma_i = D_{ij}(\omega_i)\varepsilon_j \tag{34}$$

where

$$D = \tilde{C}^{-1} \tag{35}$$

Also we need

$$R_i = -\rho \frac{\partial W}{\partial \omega_i}(\varepsilon_i, \omega_i) \tag{36}$$

$$\rho W = \frac{1}{2}[\varepsilon][D][\varepsilon] \tag{37}$$

$$dR_i = \frac{\partial R_i}{\partial \varepsilon_j} d\varepsilon_j + \frac{\partial R_i}{\partial \omega_j} d\omega_j \tag{38}$$

and

$$d\lambda = \frac{\frac{\partial f}{\partial R_k}\frac{\partial R_k}{\partial \varepsilon_j} d\varepsilon_j}{H - \frac{\partial f}{\partial R_k}\frac{\partial R_k}{\partial \omega_j}\frac{\partial f}{\partial R_j}} \tag{39}$$

The incremental form of Equation (34) is given by

$$d\sigma_i = D_{ij}\, d\varepsilon_j + \varepsilon_j \left\{ \frac{\partial D_{ij}}{\partial \omega_k} d\lambda \frac{\partial f}{\partial R_k} \right\} \tag{40}$$

$$d\sigma_i = \left\{ D_{ij} + \varepsilon_j \frac{\partial D_{ij}}{\partial \omega_k} \frac{\partial f}{\partial R_k} d\lambda \right\} d\varepsilon_j \tag{41}$$

or

$$d\sigma_i = D_{ij}^{ed}\, d\varepsilon_j \tag{42}$$

where $d\lambda$ is defined in Equation (39), and D_{ij}^{ed} is the elasto-damage stiffness matrix as defined explicitly in Equation (41). Equation (42) is useful in strain control testing.

3 APPLICATION OF PROPOSED ELASTO-DAMAGE MODEL

3.1 *Uniaxial compression*

The strain energy density $\rho\Lambda$ for uniaxial compression is given by

$$\rho\Lambda = \frac{1}{2}[\sigma \quad 0 \quad 0]\left[\tilde{C}\right]\begin{bmatrix}\sigma\\0\\0\end{bmatrix} \tag{43}$$

Substituting for the compliance $\left[\tilde{C}\right]$, and setting $\alpha = 0$ (as it is used primarily as a parameter for matching peak strengths in tension testing), one obtains

$$\rho\Lambda = \frac{\sigma^2}{2E_o} \frac{(1-\beta\omega_1)^2}{(1-\beta\omega_2)^2 (1-\beta\omega_3)^2} \tag{44}$$

The thermodynamic relation

$$\varepsilon_i = \frac{\partial(\rho\Lambda)}{\partial\sigma_i} \tag{45}$$

yields

$$\sigma = \varepsilon_1 E_o \frac{(1-\beta\omega_2)^2 (1-\beta\omega_3)^2}{(1-\beta\omega_1)^2} \tag{46}$$

Substitution of (46) in (44) yields

$$\rho W = \frac{\varepsilon_1^2 E_o}{2} \frac{(1-\beta\omega_2)^2 (1-\beta\omega_3)^2}{(1-\beta\omega_1)^2} \tag{47}$$

Using the relationship

$$R_i = -\frac{\partial(\rho\Lambda)}{\partial\omega_i} \tag{48}$$

one obtains

$$R_1 = -\frac{\beta\varepsilon_1^2 E_o (1-\beta\omega_2)^2 (1-\beta\omega_3)^2}{(1-\beta\omega_1)^3} = 0 \quad (\text{since } R_i \neq 0) \tag{49}$$

$$R_2 = \frac{\beta\varepsilon_1^2 E_o (1-\beta\omega_2)(1-\beta\omega_3)^2}{(1-\beta\omega_1)^2} \tag{50}$$

$$R_3 = \frac{\beta\varepsilon_1^2 E_o (1-\beta\omega_2)^2 (1-\beta\omega_3)}{(1-\beta\omega_1)^2} \tag{51}$$

From symmetry, $\omega_2 = \omega_3 = \omega$ and $\omega_1 = 0$ by virtue of Equation (49), yields

$$R_2 = R_3 = \beta\varepsilon_1^2 E_o (1-\beta\omega)^3 \tag{52}$$

and

$$(R_i R_i)^{1/2} = \sqrt{2}\,\beta\varepsilon_1^2 E_o (1-\beta\omega)^3 \tag{53}$$

and

$$\left[\frac{\partial f}{\partial R_i}\right] = \begin{bmatrix} 0 & \frac{1}{\sqrt{2}} & \frac{1}{\sqrt{2}} \end{bmatrix} \tag{54}$$

Differentiating R_j with respect to ω_i and ε_i and substituting along with (54) into (39) yields

$$d\lambda = \frac{2\sqrt{2}\,\beta\varepsilon_1 E_o (1-\beta\omega)^3 d\varepsilon_1}{\left(H + 3\beta^2\varepsilon_1^2 E_o (1-\beta\omega)^2\right)};$$

$$d\omega_i = d\lambda \left[\frac{\partial f}{\partial R_i}\right] \tag{55}$$

Finally, Equation (41) yields incremental stress-strain relationship for strain control testing as

$$d\sigma = \left(E_o (BW)^4 - \frac{8(\beta^2 \varepsilon_1^2 E_o^2 (BW)^6}{\left(H + 3\beta^2 \varepsilon_1^2 E_o (BW)^2\right)} \right) d\varepsilon_1 \tag{56}$$

where $BW = (1-\beta\omega)$.

Similarly, it can be shown that proceeding in a similar way incremental stress-strain relationship for stress control testing can be expressed as

$$d\varepsilon_1 = \left(\frac{1}{E_o (BW)^4} + \frac{8\beta^2\sigma^2 / (BW)^{10} * E_o^2}{\left(H - \frac{5\beta^2\sigma^2}{E_o (BW)^6}\right)} \right) d\sigma \tag{57}$$

3.2 *Uniaxial tension*

Following the same logic as in the case of uniaxial compression, it can be shown that for strain control testing,

$$d\sigma = \left(E_o (AW)^2 - \frac{4(\alpha^2 \varepsilon_1^2 E_o^2 (AW)^2}{(H + \alpha^2 \varepsilon_1^2 E_o)} \right) d\varepsilon_1 \tag{58}$$

where $AW = (1-\alpha\omega_1)$, and for stress control testing

$$d\varepsilon_1 = \left(\frac{1}{E_o (AW)^2} + \frac{4\alpha^2\sigma^2 / E_o^2 (AW)^6}{\left(H - \frac{3\alpha^2\sigma^2}{E_o (AW)^4}\right)} \right) d\sigma \tag{59}$$

3.3 *Biaxial compression*

Predictive ability of the proposed elasto-damage model for a multi-axial stress path is investigated for the biaxial stress state defined by $\sigma_1 = \sigma_2 = \sigma$. Proceeding in a manner analogous to the uni-dimensional stress state, incremental stress-strain relationship for strain control testing can be expressed as

$$d\sigma = \left(\frac{E_o (BW)^2}{(1-\nu)} - \frac{8\beta^2 \varepsilon_1^2 E_o^2 (BW)^2 / (1-\nu)^2}{\left(H + \frac{2\beta^2 \varepsilon_1^2 E_o}{(1-\nu)}\right)} \right) \times d\varepsilon_1 \tag{60}$$

and for stress control testing

$$d\varepsilon = \left(\frac{(1-\nu)}{E_o (BW)^2} + \frac{8\beta^2\sigma^2 (1-\nu)^2 / E_o^2 (BW)^6}{\left(H - \frac{6\beta^2\sigma^2 (1-\nu)}{E_o (BW)^4}\right)} \right) \times d\sigma \tag{61}$$

4 DETERMINATION OF REGRESSION COEFFICIENTS

The parameters α, β are functions of initial modulus of elasticity, E_o, uniaxial compressive strength, f_c', and normalized strain invariants, $\frac{I_1}{\varepsilon_3}$ & $\frac{J_2}{e_3^2}$. Here, ε_3 and e_3 represent the minor principal and deviatoric strain, respectively. The suggested forms of α, β are as follows:

$$\alpha = \alpha_0 (f_c', E_o) + \alpha_1 (f_c', E_o) \frac{I_1}{\varepsilon_3} + \alpha_2 (f_c', E_o) \frac{J_2}{e_3^2} + \alpha_3 (f_c', E_o) \frac{I_1}{\varepsilon_3} \frac{J_2}{e_3^2} \quad \text{(path dependent)} \tag{62}$$

or

$$\bar{\alpha} = \bar{\alpha} (f_c', E_o) \quad \text{(path independent)} \tag{63}$$

$$\beta = \beta_0 (f_c', E_o) + \beta_1 (f_c', E_o) \frac{I_1}{\varepsilon_3} + \beta_2 (f_c', E_o) \frac{J_2}{e_3^2} + \beta_3 (f_c', E_o) \frac{I_1}{\varepsilon_3} \frac{J_2}{e_3^2} \quad \text{(path dependent)} \tag{64}$$

or

$$\bar{\beta} = \bar{\beta} (f_c', E_o) \quad \text{(path independent)} \tag{65}$$

where,

$$\alpha_i = \alpha_{i1} + \alpha_{i2} f_c' + \alpha_{i3} f_c'^2 + \alpha_{i4} E_o \quad , \quad (i = 0,1,2,3) \quad \text{path dependent} \qquad (66)$$

$$\beta_i = \beta_{i1} + \beta_{i2} f_c' + \beta_{i3} f_c'^2 + \beta_{i4} E_o \quad (i = 0,1,2,3)$$

$$\bar{\alpha} = \bar{\alpha}_0 + \bar{\alpha}_1 f_c' + \bar{\alpha}_2 f_c'^2 + \bar{\alpha}_3 f_c'^3 \quad \text{path independent} \qquad (67)$$

$$\bar{\beta} = \bar{\beta}_0 + \bar{\beta}_1 f_c' + \bar{\beta}_2 f_c'^2 + \bar{\beta}_3 f_c'^3$$

These parameters were calibrated by regressing against experimental σ–ε data for different f_c'. The range of f_c' used in regression varies from 4,000 psi to 17,400 psi, and is listed in Table 1. Stress paths used in regression are listed in Table 2.

Table 1. Range of f_c' used in regression.

f_c' (psi)	E_o (10^6 psi)	ν
4000	3.605	0.19
9434	6.023	0.19
13062	6.444	0.19
17416	7.126	0.19

Table 2. Stress paths for determination of α, β.

σ_1/σ_2 for α	σ_1/σ_2 for β
–1	0
–0.25	0.2
–0.125	0.5
–0.1	0.8
–0.075	1.0
–0.05	
–0.025	

Regression was carried out in two steps as illustrated by Desai & Siriwardane (1984). In the first step, for a particular f_c' and E_o, α or β is found out to give the peak stress for different stress ratios. Then this data is regressed using the proposed form of α or β to find out α_0, α_1, α_2, α_3 or β_0, β_1, β_2, β_3. At the end of step 1 we have a set of α_i's and β_i's, where $i = 0,1,2,3$.

This process is then carried out for all the listed f_c'. The sets of α_i's and β_i's are then regressed using the proposed functional forms of α_i's and β_i's to obtain α_{i1}, α_{i2}, α_{i3}, α_{i4} or β_{i1}, β_{i2}, β_{i3}, β_{i4}.

Final form of α_i's, β_i's is as follows:

- α for path-dependent stress states

$$\alpha_0 = -(1.989E+01) + (1.788E-03) f_c' - (5.644E-08) f_c'^2 + (4.758E-07) E_o$$

$$\alpha_1 = -(3.495E+01) - (1.445E-04) f_c' + (4.415E-09) f_c'^2 + (4.593E-06) E_o \qquad (68)$$

$$\alpha_2 = (2.825E+01) - (2.561E-03) f_c' + (8.123E-08) f_c'^2 - (6.864E-07) E_o$$

$$\alpha_3 = (4.47E+01) + (4.331E-04) f_c' - (1.398E-08) f_c'^2 - (6.109E-06) E_o$$

- α for path-independent stress states

$$\bar{\alpha} = (1.116E+01) - (1.153E-03) f_c' + (3.707E-08) f_c'^2 - (1.514E-07) E_o \qquad (69)$$

- β for path-dependent stress states

$$\beta_0 = -(4.229E-02) - (2.869E-06) f_c' + (6.006E-11) f_c'^2 + (9.741E-09) E_o$$

$$\beta_1 = -(6.914E-02) + (5.829E-06) f_c' - (1.79E-10) f_c'^2 + (2.198E-09) E_o \qquad (70)$$

$$\beta_2 = (6.971E-01) - (3.09E-05) f_c' + (1.107E-09) f_c'^2 - (6.163E-08) E_o$$

$$\beta_3 = -(3.841E-01) + (1.657E-05) f_c' - (5.987E-10) f_c'^2 + (3.455E-08) E_o$$

- β for path-independent stress states

$$\bar{\beta} = (2.516E-01) - (1.978E-05) f_c' + (6.421E-10) f_c'^2 - (1.152E-08) E_o \qquad (71)$$

Depending on the state of stress (σ_1, σ_2), combinations of α, β are proposed as shown in Table 3.

5 COMPARISONS WITH EXPERIMENTAL RESULTS

Results predicted by the model discussed in the earlier sections are verified for uniaxial and biaxial loading conditions by comparing them with the available experimental results. A strain control program is used for plotting stress-strain curves

Table 3. Combinations of α, β.

State of stress	α	β
$\sigma_1 > 0$, $\sigma_2 \geq 0$	$\bar{\alpha}(f_c', E_o)$	0
$\sigma_1 > 0$, $\sigma_2 < 0$	$\alpha\left(f_c', E_o, \frac{I_1}{\varepsilon_3}, \frac{J_2}{e_3^2}, \frac{I_1}{\varepsilon_3} * \frac{J_2}{e_3^2}\right)$	$\bar{\beta}(f_c', E_o)$
$\sigma_1 \leq 0$, $\sigma_2 < 0$	0	$\beta\left(f_c', E_o, \frac{I_1}{\varepsilon_3}, \frac{J_2}{e_3^2}, \frac{I_1}{\varepsilon_3} * \frac{J_2}{e_3^2}\right)$

for different loading conditions.

For the case of uniaxial compression, stress-strain curves are plotted for three different concretes (concrete A, f_c' = 4000 psi (Fig. 1); concrete B, f_c' = 9434 psi (Fig. 2); concrete C, f_c' = 17,416 psi (Fig. 3)). Comparison with experimental results (Wee et al. 1996, Wischers 1978) shows that the peak stress obtained analytically matches with the experimental results quite well, but the strain is somewhat smaller than the experimental values for concrete A and B. Also, the predicted stress-strain curves show less ductility for concrete A and B, while for concrete C the curve matches quite well with the experimental result. This can be attributed to the absence of plastic strains. Additional plastic strains will shift the curves to the right, making the strains match with the experimental results. Increasing brittleness and decreasing ductility have been predicted reasonably well as can be seen for concrete C.

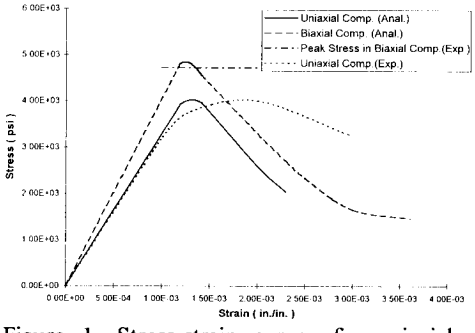

Figure 1. Stress-strain curves for uniaxial and biaxial compression (f_c' = 4000 psi).

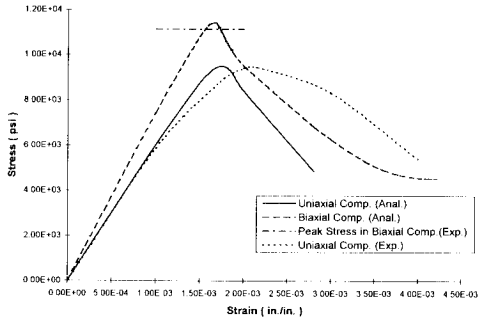

Figure 2. Stress-strain curves for uniaxial and biaxial compression (f_c' = 9434 psi).

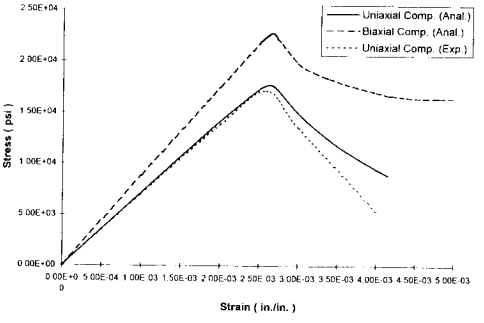

Figure 3. Stress-strain curves for uniaxial and biaxial compression (f_c' = 17,416 psi).

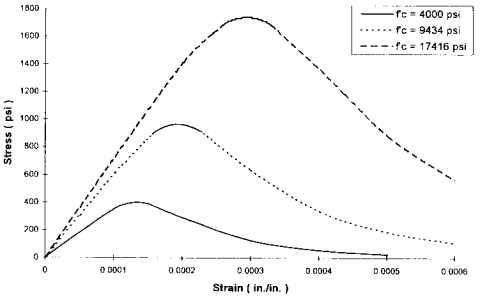

Figure 4. Stress-strain curves for uniaxial tension.

For the case of uniaxial tension, shape of the stress-strain curves (softening in post-peak zone), Figure 4, compares well with the experimental results of Gopalaratnam and Shah (1985).

For the case of biaxial compression, comparison with experimental results of Kupfer et al. (1969), Figures 5-7, indicates that the predicted peak stress is somewhat higher, but is in the range as predicted

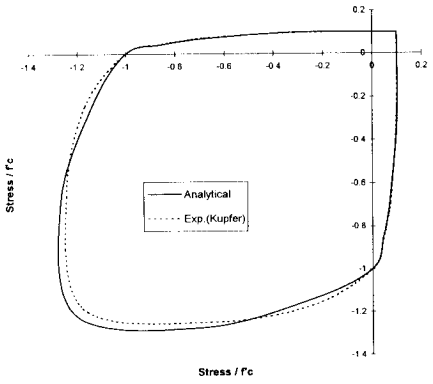

Figure 5. Biaxial strength interaction curve for concrete (f_c' = 4000 psi).

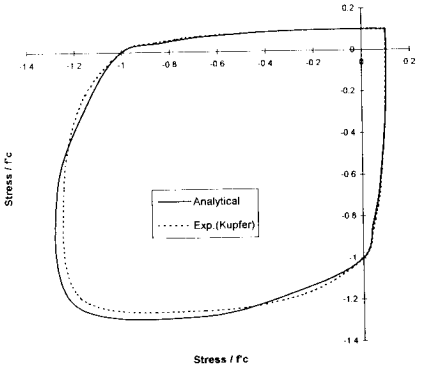

Figure 6. Biaxial strength interaction curve for concrete (f_c' = 9434 psi)

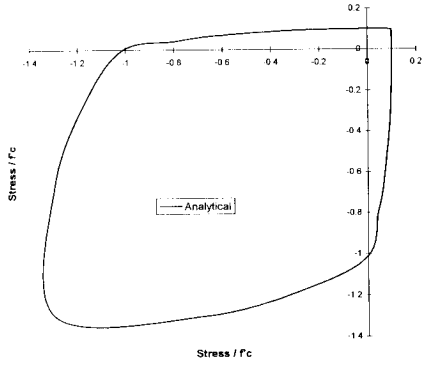

Figure 7. Biaxial strength interaction curve for concrete (f_c' = 17,416 psi)

by Linhua et al. (1991). Biaxial strength interaction envelope is plotted for all three concretes, which compares very well with the envelope as predicted by Kupfer et al. (1969).

6 CONCLUSIONS

An elasto-damage bounding surface model for the monotonic behavior of normal and high strength concrete is developed in this paper. A generalized compliance matrix is developed in the principal coordinate system by introducing damage effect tensor $\underline{M}(\omega)$, which takes into account the different behavior of concrete in tension and compression by introducing two new parameters α and β.

The stress-strain curves and biaxial strength interaction envelope presented in this paper demonstrate that the proposed model predicts the behavior of concrete under multiaxial monotonic loading adequately. The proposed model predicts the essential features of concrete quite well except for volumetric dilatation. Since plastic strains are not considered here, predicted stress-strain curves are stiffer than experimental curves. It is therefore recommended to include the effect of plastic deformation in modelling the behavior of concrete.

In order to make the model general and applicable to real three dimensional problems, more triaxial data needs to be incorporated in determining the regression coefficients. Work is in progress in this direction.

ACKNOWLEDGEMENT

The authors are indebted to the Department of Civil Engineering, King Fahd University of Petroleum & Minerals, for their support in the pursuit of this work.

REFERENCES

Abu-Lebdeh, T.M. & G.Z. Voyiadjis 1993. Plasticity-damage model for concrete under cyclic multiaxial loading. *J. Engg. Mech.*, ASCE 119(7): 1465-1484.

Chow, C.L. & J. Wang 1987a. An anisotropic theory of elasticity for continuum damage mechanics. *Int. J. Fracture* 33: 3-16.

Chow, C.L. & J. Wang 1987b. An anisotropic theory of continuum damage mechanics for ductile fracture. *Engg. Fract. Mech.* 27(5): 547-558.

Cordebois, J.P. & F. Sidoroff 1982. Anisotropic damage in elasticity and plasticity. *J. Méc.*

Théor. Appl., Numéro Spécial: 45-60 (in French).

Dafalias, Y.F. & E.P. Popov 1977. Cyclic loading for material with a vanishing elastic region. *Nucl. Engg. Design* 44: 293-302.

Desai, C.S. & H.J. Siriwardane 1984. *Constitutive laws for engineering materials with emphasis on geologic materials.* Englewood Cliffs, N.J.: Prentice-Hall, Inc.: 114-120.

Fardis, M.N., B. Alibe & J.L. Tassoulas 1983. Monotonic and cyclic constitutive law for concrete. *J. Engg. Mech.*, ASCE 109(2): 516-536.

Gopalaratnam, V.S. & S.P. Shah 1985. Softening response of plain concrete in direct tension. *ACI Journal* 82(3): 310-323.

Kachanov, L.M. 1958. Time of the rupture process under creep conditions. *Izv Akad. Nauk*, U.S.S.R., Otd. Tekh. Nauk 8: 26-31.

Kupfer, H., H.K. Hilsdorf & H. Rusch 1969. Behavior of concrete under biaxial stresses. *ACI Journal Proc.*, 66(8): 656-666.

Linhua, J., H. Dahai & X. Nian Xing 1991. Behavior of concrete under triaxial compressive-compressive-tensile stresses. *ACI Materials J.* 88(2): 181-185.

Suaris, W., C. Onyang & V.M. Fernando 1990. Damage model for cyclic loading of concrete. *J. Engg. Mech.*, ASCE 116(5): 1020-1035.

Voyiadjis, G.Z. & T.M. Abu-Lebdeh 1993. Damage model for concrete using bounding surface concept. *J. Engg. Mech.*, ASCE 119(19): 1865-1885.

Wee, T.H., M.S. Chin & M.A. Mansur 1996. Stress-strain relationship of high-strength concrete in compression. *J. Matls. Civil Engg.* 8(2): 70-76.

Wischers, G. 1978. Application of effects of compressive loads on concrete. *Beton Technische Berichte* No. 2 & 3, Duesseldorf, Germany.

Yazdani, S. & H.L. Schreyer 1990. Combined plasticity and damage mechanics model for plain concrete. *J. Engg. Mech.*, ASCE 116(7): 1435-1450.